Electronic Supplementary Information

Experimental section

Materials: $Na_2MoO_4·2H_2O$, $(NH_4)_6Mo_7O_{24}·4H_2O$, $Co(NO_3)_2·6H_2O$, KOH and $CoCl_2·6H_2O$ were purchased from Chengdu Kelon Chemical Reagent Factory. $RuCl_3·3H_2O$ and a Nafion (5 wt%) solution were bought from Sigma-Aldrich Chemical Reagent Co., Ltd. All the reagents were used as received without further purification. Ni foam was bought from Beijing Xinxing Bairi Technology Co., Ltd. Prior to use, the Ni foam (1 cm*3 cm) was pre-cleaned in an ultrasonic bath of acetone for 15 min to remove any greasy spats. Then, it was immersed in 3 M HCl solution for 10 min to eliminate the surface oxide layer. At last, it was washed with deionized water and ethanol for 3 times, respectively. The water purified through a Millipore system was used throughout whole progress.

Preparation of $CoMoO_4$ NP@PAs/NF: Firstly, CoMo-precursor NPAs/NF was synthesized according to previous work with slight modification.[1] In a typical synthesis, 1.25 mmol of $Co(NO_3)_2·6H_2O$ and 1.25 mmol of $Na_2MoO_4·2H_2O$ was added to 40 mL water under vigorous stirring for 15 min. Then the clear solution was poured into a Teflon-lined stainless autoclave and a piece of Ni foam was immersed into the solution. The autoclave was sealed and maintained at 180 °C in an electric oven for 12 h. When the autoclave cooled down naturally to room temperature, the Ni foam coated with CoMo-precursor NPAs/NF was rinsed by water and ethanol for 3 times. Secondly, a piece of as-prepared CoMo-precursor NPAs/NF was placed against the wall of a Teflon-lined stainless-steel autoclave which containing a homogeneous solution of $CoCl_2·6H_2O$ (1 mmol) and $(NH_4)_6Mo_7O_{24}·4H_2O$ (1 mmol) in a solvent of 20 ml of H_2O. After the autoclave was sealed and maintained at 150 °C for 5 h and cooled to room temperature, it was taken out and washed by water and ethanol for 3 times and then dried at 60 °C overnight under Ar to obtain CoMo-precursor NP@PAs/NF. At last, CoMo-precursor NP@PAs/NF was calcined at 300 °C for 3 h with a temperature ramp rate of 2 °C min^{-1} in Ar atmosphere to get $CoMoO_4$ NP@PAs/NF. For comparison, $CoMoO_4$ NPAs/NF was also synthesized by calcining

CoMo-precursor NPAs/NF at 300 °C for 3 h with a temperature ramp rate of 2 °C min^{-1} in argon atmosphere. To explore the impact of second hydrothermal reaction time on morphology and catalytic performance of electrocatalyst, the samples in second hydrothermal process were taken out at different times(3, 5, 7h).

Preparation of $CoMoO_4$ Powder/NF: $CoMoO_4$ powder precursor were prepared by a hydrothermal progress used in the preparation of $CoMoO_4$ NP@PAs/NF. In brief, a homogeneous solution of $CoCl_2 \cdot 6H_2O$ (1 mmol) and $(NH_4)_6Mo_7O_{24} \cdot 4H_2O$ (1 mmol) in a solvent of 20 ml of H_2O were sealed in a autoclave, and then maintained at 150 °C for 5 h. When the autoclave cooled down naturally to room temperature, the sediment was rinsed by water and ethanol for 3 times, followed by drying in 60 °C overnight under Ar. $CoMoO_4$ powder were obtained after annealed at 300 °C for 3 h in argon atmosphere. The as-prepared $CoMoO_4$ powder (0.01 g) was dispersed into a solution of Nafion, ethanol and water with a volume ratio of 10/250/250 via sonication, and deposited onto NF with a loading of 4.3 mg cm^{-2}.

Synthesis of RuO_2/NF: RuO_2 was prepared according to previous publication.[2] Briefly, 2.61 g of $RuCl_3 \cdot 3H_2O$ and 30 mL KOH (1 M) were added into 100 mL distilled water and stirred for 45 min at 100 °C. Then the above solution was centrifuged for 10 minutes and filtered. The precipitates were collected and washed with water several times. Finally, the product was dried at 80 °C overnight and then annealed at 350 °C in air atmosphere for 1 h. At last, the as-prepared RuO_2 was deposited onto NF with a loading of 4.3 mg cm^{-2} by the same method for $CoMoO_4$ nanoparticles.

Characterizations: Panaiytical/Empyrean diffractometer with Cu Kα radiation (λ=1.5418 Å) was used for X-ray diffraction (XRD). A XL30 ESEM FEG scanning electron microscope was employed for scanning electron microscope (SEM) by an accelerating voltage of 20 kV. Transmission electron microscopy (TEM) images were taked by a HITACHI H–8100 electron microscopy with an accelerating voltage of 200 kV. For obtaining X-ray photoelectron spectroscopy (XPS) data, an ESCALABMK II X-ray photoelectron spectrometer with excitation source of Al was used.

Electrochemical measurements: Electrochemical measurements were performed with a RST electrochemical workstation (Zhengz-hou Shiruisi Technology Co., Ltd.) in a standard three-electrode setup with a $CoMoO_4$ NP@PAs/NF-5h as the working electrode. A platinum plate and an Hg/HgO were used as the counter electrode and the reference electrode, respectively. All electrochemical measurements were carried out at room temperature (298.15 K) *via* the adjustment of air condition and heating support, ensuring the variation of diffusion coefficient within 1%, and all potentials reported in this work were calibrated to RHE unless especially stated according to the following equation: E (RHE) = E (Hg/HgO) + (0.098+ 0.059 pH) V.

Turnover frequency (TOF) calculations: For TOF calculation, we need to electrochemically quantify the surface concentration of redox Co and Mo species at first. A linear relationship between the plot of the oxidation peak current densities for redox Co and Mo species and scan rates can be derived from the electrochemical cyclic voltammograms according to the following equation in previous report[3]:

$$\text{Slope} = n^2F^2A\Gamma_0/RT$$

Where n for the number of electrons transferred is 1 assuming a one-electron process for oxidation of Co and Mo centers in $CoMoO_4$ NP@PAs-5h; F representing Faraday's constant is 96485 C mol^{-1}; A is the geometrical surface area of the electrode (0.25 cm^2); Γ_0 is the surface concentration of active sites (mol cm^{-2}), and R and T are the ideal gas constant and the absolute temperature, respectively.

Then, TOF values can be calculated based on the formula below:

$$\text{TOF} = jA/4Fm$$

Where j is the current density, 4 indicates the mole of electrons consumed for one mole of O_2 evolution, and m is the mole number of active sites.[4]

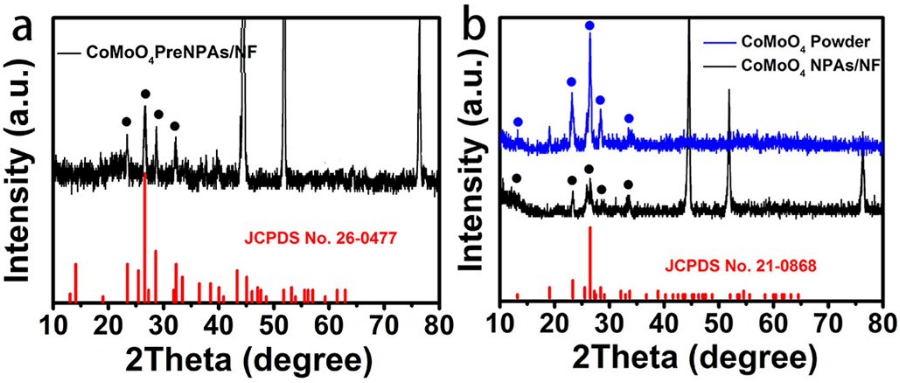

Fig. S1. XRD patterns for (a) $CoMoO_4$ PreNPAs/NF, (b) $CoMoO_4$ Powder/NF and $CoMoO_4$ NPAs/NF.

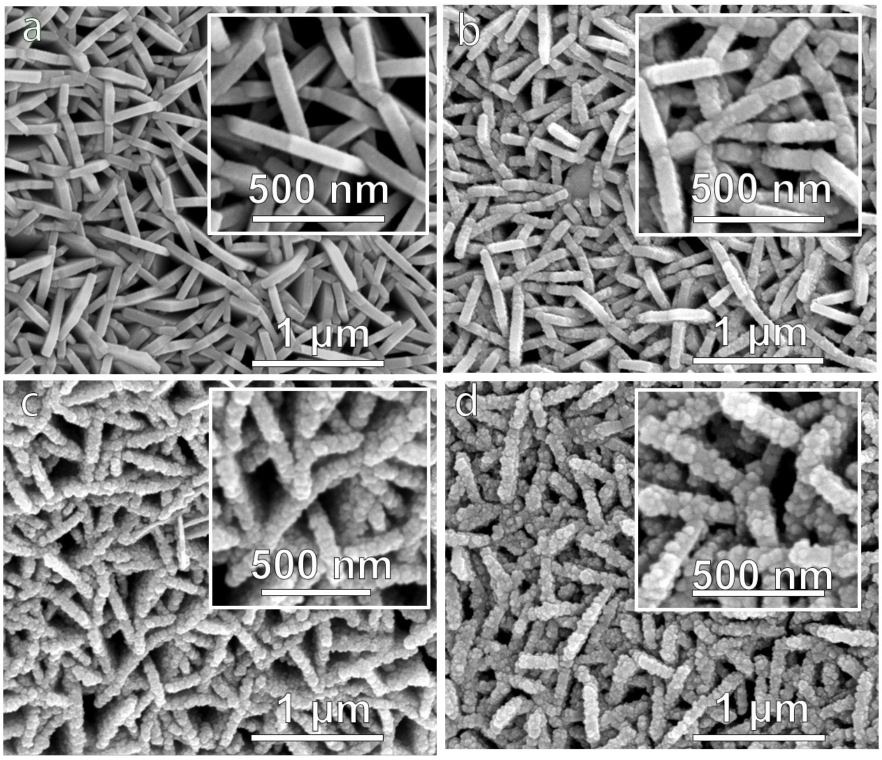

Fig. S2. SEM images for (a) $CoMoO_4$ NPAs/NF, $CoMoO_4$ NP@PAs/NF in second hydrothermal reaction times of 3 h (b), 5 h (c) and 7 h (d).

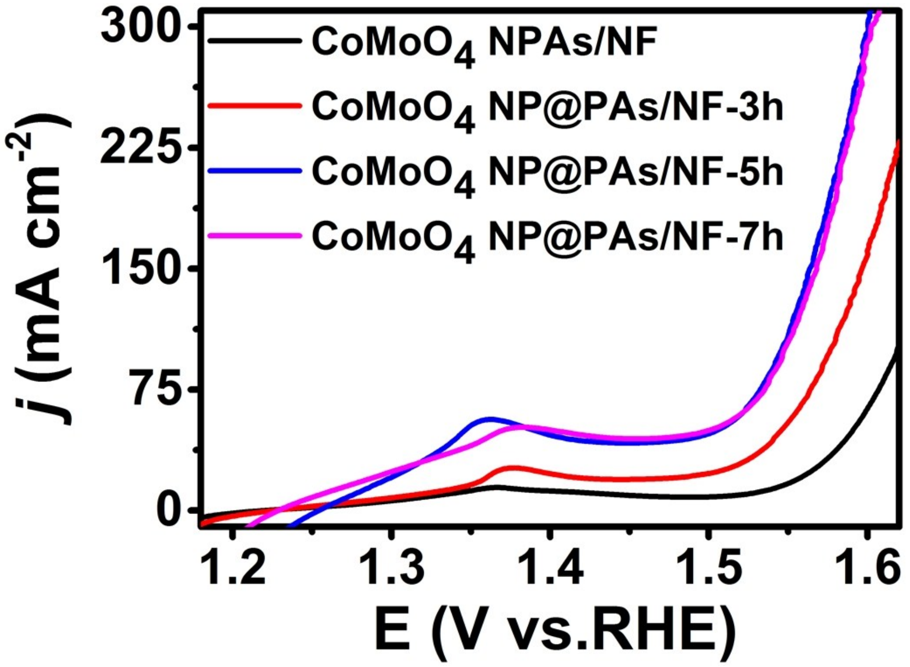

Fig. S3. LSV curves for CoMoO$_4$ NPAs/NF, CoMoO$_4$ NP@PAs/NF in different second hydrothermal reaction time.

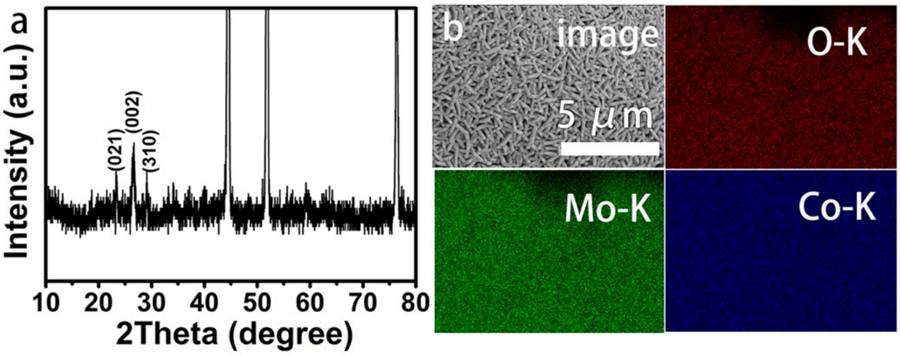

Fig. S4. (a) XRD pattern, (b) SEM image and corresponding EDX elemental mapping images for $CoMoO_4$ NP@PAs/NF after 25-hours durability test.

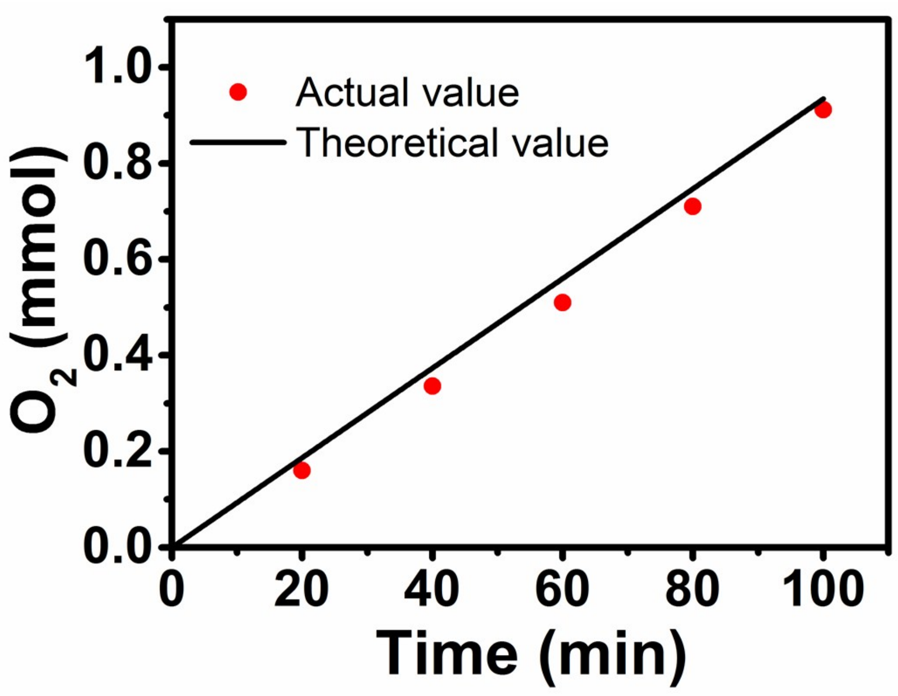

Fig. S5. The amount of oxygen theoretically calculated and experimentally measured vs. time for $CoMoO_4$ NP@PAs/NF in 1 M KOH.

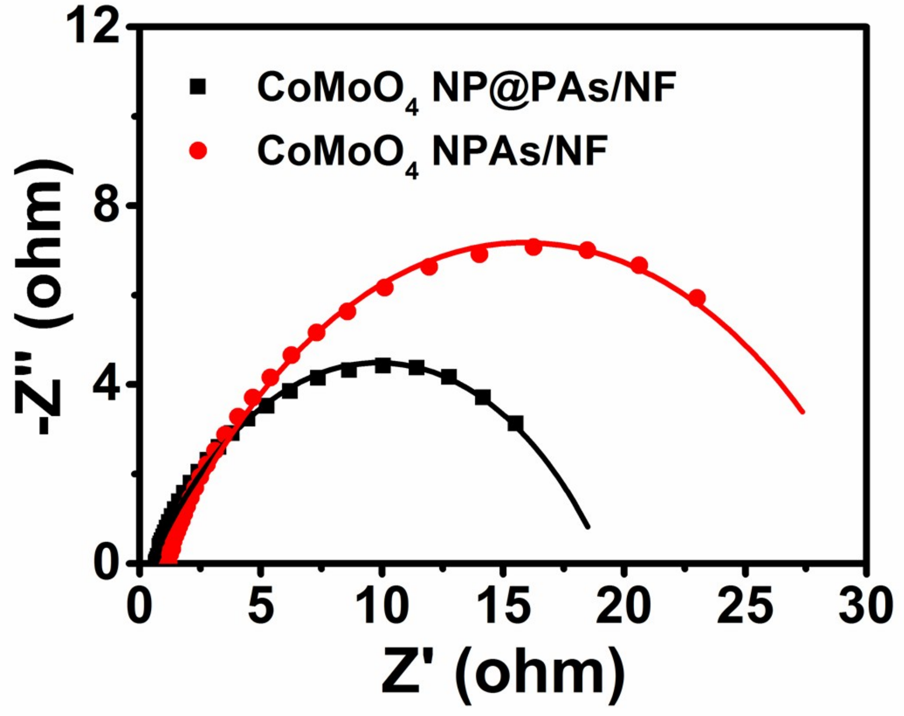

Fig. S6. Nyquist plots of CoMoO$_4$ NPAs/NF and CoMoO$_4$ NP@PAs/NF in a frequency ranging from 0.01 to 10^5 Hz with the fitting curves.

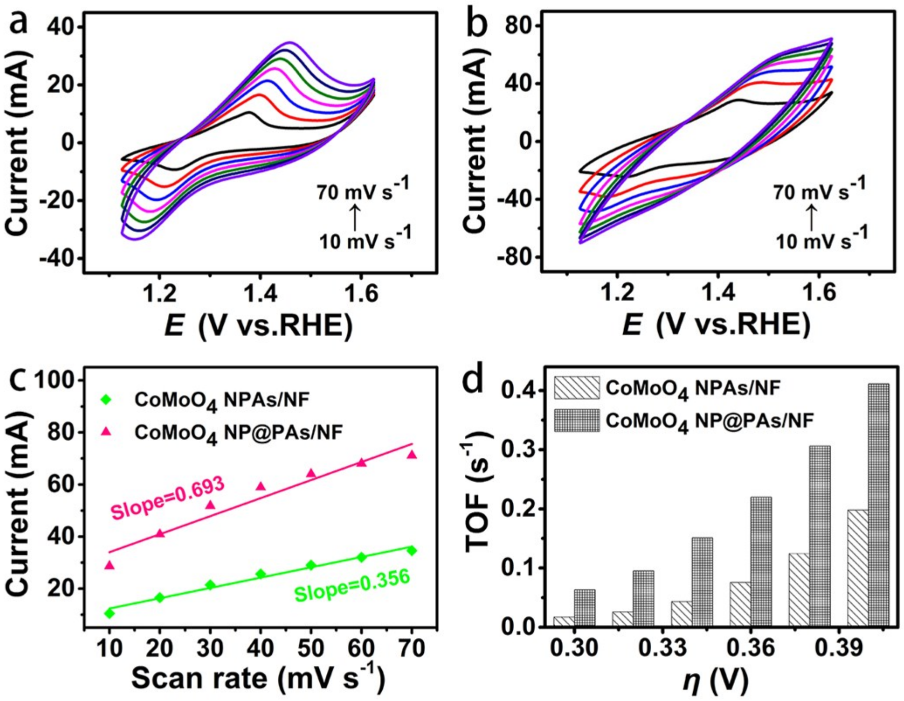

Fig. S7. CV for (a) $CoMoO_4$ NPAs/NF and (b) $CoMoO_4$ NP@PAs/NF in the faradic capacitance current range of 1.125-1.625 V at scan rates from 10 to 70 mV s^{-1} in 1 M KOH. (c) Plots of oxidation peak current densites versus the scan rates from CVs in 1 M KOH for $CoMoO_4$ NPAs/NF and $CoMoO_4$NP@PAs/NF. (d) TOF values for $CoMoO_4$ NPAs/NF and $CoMoO_4$ NP@PAs/NF at different fixed overpotentials.

Table S1. Comparison of water oxidation performance for $CoMoO_4$ NP@PAs/NF with other metal molybdates electrocatalysts.

Catalyst	**J (mA cm^{-2})**	**η (mV)**	**Electrolyte (KOH)**	**Ref.**
$CoMoO_4$ NP@PAs/NF-5h	50	272	1 M	This work
	100	317		
$FeMoO_4$/NF	50	293	1 M	4
	100	321		
$CoMoO_4$-$Ni(OH)_2$/NF	100	349	1 M	5
N-$NiMoO_4$/ NiS_2	100	335	1 M	6
Co_3O_4/$CoMoO_4$ nanocages	10	318	1 M	7
$NiMoO_4$ nanorods	10	340	1 M	8
$CoMoO_4$/CC	50	320	1 M	9
$CoMoO_4$@$Ni(OH)_2$ nanocubes	10	350	1 M	10
$CoMoO_4$ nanorods	10	343	1 M	11
β-$NiMoO_4$	10	300	1 M	12
$Ni_{0.9}Fe_{0.1}MoO_4$	10	299	1 M	13

References

1. D. Guo, H. Zhang, X. Yu, M. Zhang, P. Zhang, Q. Li and T. Wang, *J. Mater. Chem. A*, 2013, **1**, 7247.
2. G. Zhu, L. Yang, R. Zhang, F. Qu, Z. Liu, G. Du, A. M. Asiri, Y. Yao and X. Sun, *Nanoscale*, 2017, **9**, 12343-12347.
3. Y. Li, L. Zhang, X. Xiang, D. Yan and F. Li, *J. Mater. Chem. A*, 2014, **2**, 13250–13258.
4. Y. Gou, Q. Liu, Z. Liu, A. M. Asiri, X. Sun and J. Hu, *Inorg. Chem. Front.*, 2018, **5**, 665-668.
5. Y. Xu, L. Xie, D. Li, R. Yang, D. Jiang and M. Chen, *ACS Sustain. Chem. Eng.*, 2018, **6**, 16086-16095.
6. L. An, J. Feng, Y. Zhang, R. Wang, H. Liu, G.-C. Wang, F. Cheng and P. Xi, *Adv. Funct. Mater.*, 2019, **29**, 1805298.
7. L. Zhang, T. Mi, M. A. Ziaee, L. Liang and R. Wang, *J. Mater. Chem. A*, 2018, **6**, 1639-1647.
8. X. Zhao, J. Meng, Z. Yan, F. Cheng and J. Chen, *Chin. Chem. Lett.*, 2019, **30**, 319-323.
9. F. Wang, J. Zhao, W. Tian, Z. Hu, X. Lv, H. Zhang, H. Yue, Y. Zhang, J. Ji and W. Jiang, *RSC Adv.*, 2019, **9**, 1562-1569.
10. X. Wang, F. Rong, F. Huang, P. He, Y. Yang, J. Tang and R. Que, *J. Alloys Compd.*, 2019, **789**, 684-692.
11. X. Liu, Y. Yang and S. Guan, *Chem. Phys. Lett.*, 2017, **675**, 11-14.
12. S. Ratha, A. K. Samantara, K. K. Singha, A. S. Gangan, B. Chakraborty, B. K. Jena and C. S. Rout, *ACS Appl. Mater. Interfaces*, 2017, **9**, 9640-9653.
13. J. Chen, G. Zhao, Y. Chen, K. Rui, H. Mao, S. X. Dou and W. Sun, *Chem-Eur. J.*, 2019, **25**, 280-284.